

# Observation of ELM structures in MAST and AUG using a fast camera

B. Koch <sup>\*</sup>, A. Herrmann, A. Kirk, H. Meyer, J. Dowling, J. Harhausen, J. Neuhauser, H.W. Müller, W. Bohmeyer, G. Fussmann, AUG Team, MAST Team

*MPI für Plasmaphysik, EURATOM Association, Garching, Germany  
EURATOM/UKAEA Fusion Association, Culham Science Centre, England, United Kingdom*

---

## Abstract

Edge localised modes (ELMs) are repetitive instabilities that occur in the outer region of tokamak plasmas. In this work, for the first time, we present image sequences of the temporal evolution of the observed filamentary structures during the ELM events.

© 2007 Elsevier B.V. All rights reserved.

*PACS:* 52.40.Hf; 52.55.Fa

*Keywords:* ELM; MAST; ASDEX Upgrade

---

## 1. Introduction

One of the key issues of forthcoming fusion experiments (ITER, DEMO) is the high energy flux density to the divertor components and the first wall. Even with a careful choice of geometry and materials, the projected peak loads are close to the damage threshold leaving only a very narrow safety margin.

In large part this peak energy load is brought forth by periodically occurring instabilities within the plasma edge, so called edge localized modes or

ELMs. These ELMs are a frequently observed phenomenon for tokamak discharges operating in the high confinement mode (H-mode) [1,2]. During the ELM, a substantial fraction of the energy stored in the core plasma (5–15%) is suddenly released into the scrape-off layer in a short amount of time (100–300  $\mu$ s) resulting in a drastically increased heat load to the plasma facing components. At the same time, this brief degradation of confinement helps to dispose of impurity ions, e.g. helium or tungsten, thus counteracting impurity accumulation. Therefore, a detailed understanding of the underlying physics of ELMs is required in order to exploit this positive feature while complying with the engineering limits.

Within the scrape-off layer, ELMs manifest themselves as filamentary approximately field aligned

---

<sup>\*</sup> Corresponding author. Address: MPI für Plasmaphysik, EURATOM Association, Garching, Germany. Fax: +49 30 2093 7549.

*E-mail address:* [bernd.koch@ipp.mpg.de](mailto:bernd.koch@ipp.mpg.de) (B. Koch).

structures [3,4]. These filaments have been observed in a wide range of tokamaks and have been studied using a number of diagnostics including magnetic measurements, target plate thermography, electrical probes and single frame optical images. For the first time, in this work we present the temporal evolution of the observed filamentary structures during the ELM events. The experiments were conducted in ASDEX Upgrade and MAST using a fast camera in the visible spectral range. By its design, this camera is capable of recording up to six frames during an individual ELM. In the images filamentary structures are clearly visible and can be compared with projections of field lines calculated using an equilibrium code. Based on this comparison the position and width of individual filaments as well as the mode number can be determined. Combining data from successive frames it is possible to estimate the rotation speed and the radial expansion of the filaments.

This article is structured as follows: the current section is followed by a description of the experimental setup at MAST and ASDEX Upgrade and the method used to obtain three dimensional data from the images. After this, the experimental results are presented and discussed. And, finally, the most important aspects will be summarized.

## 2. Experimental setup and evaluation of the data

In both experiments a fiber optic image guide was used to connect the camera (a Hadland Imacon) to the objective used. At the MAST tokamak the plasma was viewed through an observation port located in the midplane. In combination with the wide angle lens used and the low aspect ratio of the device it was possible to view the entire plasma

(see Fig. 1). Although the camera was operated without a spectral filter, most of the observed light originates from the deuterium  $D_\alpha$  transition. In order to obtain a trigger signal, the current to the divertor plates was monitored. It was found that just on the verge of the ELM (characterized by the rise of the intensity of the  $D_\alpha$  emission) a pronounced negative current peak occurs which could be successfully utilized as a reliable trigger source. Following the trigger signal each of the six frames was consecutively exposed for a period between 15 and 40  $\mu\text{s}$  within the first 200  $\mu\text{s}$  of the ELM. The results presented herein are based on sets of six images from eight type-I ELMs obtained in connected double null discharges with a plasma current of 750 kA, 1.8 MW of neutral beam heating and a line averaged density of  $4 \times 10^{19} \text{ m}^{-3}$ .

At ASDEX Upgrade, the camera was connected to a lens mounted in the upper part of the vessel aimed at the upper divertor (see Fig. 1). The trigger signal was derived from the current to one of the probe tips embedded into the divertor plates. The measurements were performed on two type-I ELMs observed in upper single null discharges with a plasma current of 800 kA, a total heating power of 6.9 MW and a line averaged density of  $7 \times 10^{19} \text{ m}^{-3}$ .

For the purpose of determining the toroidal and radial position of the filaments a well established method for the evaluation of images from surveillance cameras was used [5]: first, the exact viewing geometry was determined from observed contours of in-vessel components. The filaments were then superimposed with two dimensional projections of magnetic field lines calculated using an equilibrium code. These field lines were calculated starting out from different radial positions in the midplane.

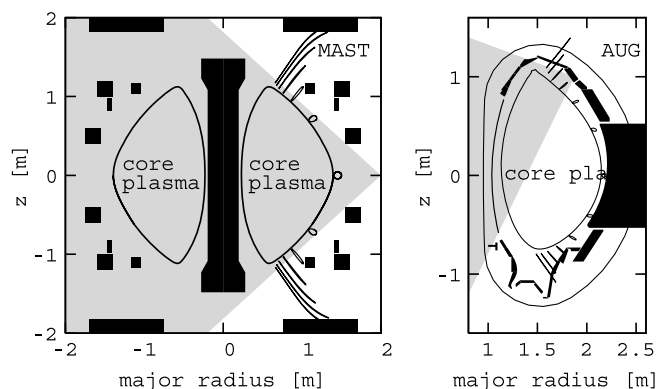


Fig. 1. Poloidal cross-sections of core plasma and of an exemplary flux tube (filament) at MAST (left) and ASDEX Upgrade (right). The cross-section of the flux tube is given at toroidal intervals of  $60^\circ$ . The shaded areas indicate the field of vision.

Subsequently, the field line with the most suitable starting point was brought into agreement with the filament by rotating it around the center of the torus. The values specified here are the radial ( $r$ ) and toroidal ( $\phi$ ) location of the filament in the mid-plane. The toroidal angle  $\phi$  is defined such that  $0^\circ$  ( $360^\circ$ ) is at the back,  $90^\circ$  at the left hand edge,  $180^\circ$  at the front and  $270^\circ$  at the right hand side of the pictures. The process of evaluation is illustrated in one of the frames depicted in Fig. 2.

Applying sections at different positions in the image as depicted in the same figure, the position as well as the width of the filament can be determined with an accuracy of  $\pm 2$  cm radially and  $\pm 2^\circ$  toroidally. However, it has to be noted that the accuracy of the obtained values strongly depends on the position of the filament: the radial position can be most directly determined for filaments showing at the left or right hand side in the midplane. In this case, the toroidal position is obtained by matching the parts of the filament approaching the upper and lower X-points. For filaments showing at the front or at the back the situation is reversed: the toroidal position can be determined in the midplane while the radial information must be inferred from the tail.

For the interpretation of the data it is also essential to consider the cross-section of the filaments as well as the field of view as indicated by the shaded area in Fig. 1. Assuming a circular shape of the filament at the midplane, traveling along its length

towards the X-point and the divertor the filament is distorted into a thin, elongated sheath (This also accounts for stripe like energy deposition patterns observed by divertor thermography [6]). As a consequence, approaching the X-point it becomes impossible to distinguish between the individual filaments.

### 3. Experimental results and discussion

Due to the advantageous viewing geometry, the most useful information about the filamentary structures can be obtained from the measurements performed at MAST. Some exemplary pictures are provided in Fig. 2. Usually, a number of 5–10 filaments with an toroidal extent of  $\approx 4^\circ$  and a radial size of 5–10 cm can be observed. Comparing the number of observed filaments with a mode number derived from the minimum toroidal spacing, the latter turns out to be up to a factor of two higher. While this could be explained by assuming that some filaments have an elevated temperature and, consequently, cannot be observed in the visible spectral range, two other findings suggest that the filamentary structures are not truly periodic in  $\phi$ : firstly, the individual filaments can be located at different radial positions. Secondly, some filaments (especially those with larger  $r$ ) show an individual motion: while they stop rotating toroidally they accelerate radially. We suggest that the reason for this behavior can be found in the initial phase of

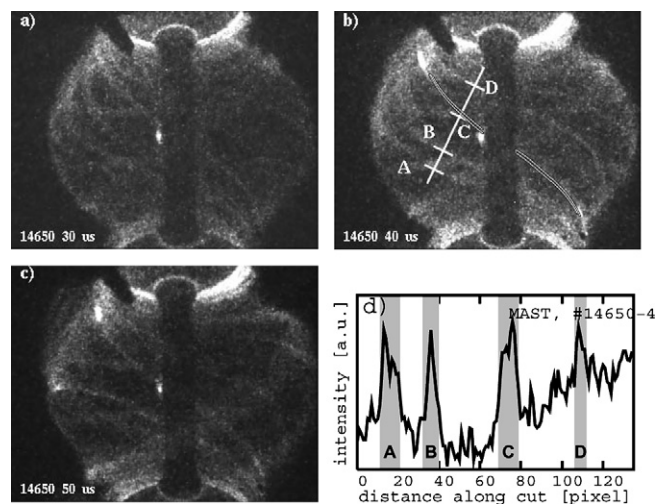


Fig. 2. Exemplary image sequence of a type-I ELM at MAST (a–c). The subsequent pictures were taken with an exposure time of  $10 \mu\text{s}$ . The second frame (b) has been overlaid with a projection of a magnetic field line and a straight line indicating the location of the line cut shown in (d).

the ELM: originally, the ELM develops as a MHD-instability with a given mode number. After this, at some positions flux tubes with increased plasma density separate from the core plasma. This is a local process and these flux tubes can be observed as filaments. Finally, the filament totally loses its connection to the core plasma and its toroidal rotation and accelerates radially outwards.

An example of the motion of an individual filament is given in Fig. 3: in the initial frame, the filament is located just outside the last closed flux surface at  $r = 1.46$  m. Between the first and the second frame the filament moves with a toroidal

speed of  $v_t = 13$  km/s, a value which is consistent with the rotation velocity of the pedestal, while essentially maintaining its radial position. Subsequently, it first slows down toroidally and then also starts to accelerate radially. In Fig. 3, two different values are provided for the radial acceleration. For the lower value,  $a_r = 1 \times 10^8$  m/s<sup>2</sup>, the radial motion is assumed to already start at the first frame, for the higher value,  $a_r = 7 \times 10^8$  m/s<sup>2</sup>, at the fourth frame only.

At ASDEX Upgrade, similar field aligned structures could be observed (see Fig. 4). However, it was not possible to follow individual filaments through several frames in order to determine their velocity. Instead, the structures appear at random positions in each frame without temporal correlation. Although it cannot be excluded that the observed structures are simply flux tubes highlighted by enhanced erosion at tile edges or other component structures, this is most likely due to the small gap between the last closed flux surface and the wall ( $\approx 5$  cm) which is comparable to the filament size. Taking into account the time of exposure  $\tau = 40 \mu\text{s}$ , it is possible to give a lower limit for the radial velocity of the filament: structures moving faster than  $v_r \approx 1300$  m/s cross the distance between the plasma edge and the wall during the exposure time and, consequently, only show on a single frame. In this case, the apparent size of the structure in the image is determined by the gap size.

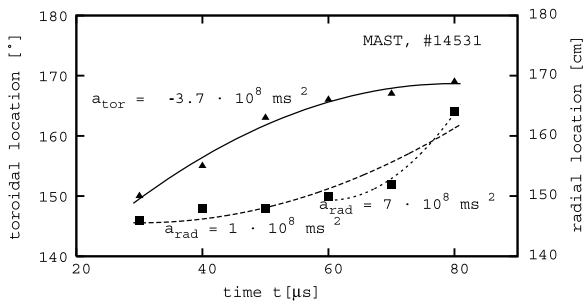


Fig. 3. Toroidal (triangles) and radial (squares) position of an individual filament from Fig. 2 as functions of time. For toroidal motion, the solid line indicates a continuous deceleration towards  $v_{tor} = 0$  at  $t = 80 \mu\text{s}$ . In case of the radial expansion, two fit curves are given: a continuous acceleration from  $t = 0 \mu\text{s}$  (dashed) as well as an accelerated movement starting not until  $t = 60 \mu\text{s}$  (dotted).

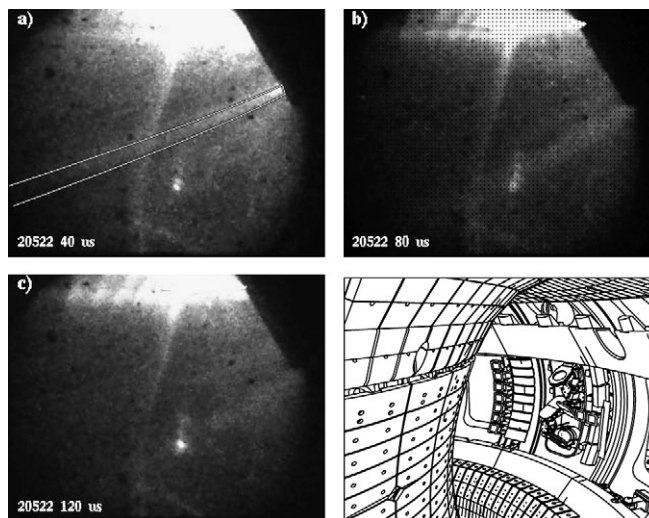


Fig. 4. Exemplary image sequence of a type-I ELM at ASDEX Upgrade (a–c). For the first frame, the two lines indicate the location of a filament. In order to ease the interpretation of the pictures, a CAD drawing of the vessel and the in-vessel components as seen by the camera is also provided.

#### 4. Summary

In this work we have presented unique high speed picture sequences of filamentary structures in the scrape-off layer of the MAST and ASDEX Upgrade tokamaks during type-I ELMs. The observed structures are field aligned and have quasi mode numbers 5–10, although the periodicity is not exact. If the clearance between the last closed flux surface and the nearest wall is sufficiently large it is possible to follow individual filaments. The observed velocities change with time. Filaments start out with high toroidal velocities of the order of  $10^4$  m/s, slow down to about  $10^3$  m/s and move radially outward

with an acceleration of the order of  $10^8$  m/s<sup>2</sup>. This accelerated motion could possibly be driven by the  $\mathbf{E} \times \mathbf{B}$  drift which is of similar magnitude, but further studies will be required to clarify this. Proceedings.

#### References

- [1] J.W. Connor, Plasma Phys. Control. Fus. 40 (1998) 531.
- [2] A. Loarte et al., Plasma Phys. Control. Fus. 44 (2002) 1815.
- [3] A. Kirk et al., Plasma Phys. Control. Fus. 47 (2005) 995.
- [4] A. Kirk et al., Phys. Rev. Lett. 96 (2006) 185001.
- [5] G.S.K. Fung et al., Opt. Eng. (Bellingham, Wash.) 42 (2003) 2967.
- [6] T. Eich, Plasma Phys. Control. Fus. 47 (2005) 815.